analytical chemistry

pubs.acs.org/ac Article

Integration of NMR Spectroscopy in an Analytical Workflow to Evaluate the Effects of Oxidative Stress on Abituzumab: Beyond the Fingerprint of mAbs

Linda Cerofolini, Enrico Ravera, Christian Fischer, Andrea Trovato, Francesca Sacco, Wolf Palinsky, Gabriella Angiuoni, Marco Fragai,* and Fabio Baroni*

Cite This: *Anal. Chem.* 2023, 95, 9199−9206 Read Online

ACCESS | Metrics & More | Article Recommendations | Supporting Information

ABSTRACT: The assessment of the higher-order structure (HOS) by NMR is a powerful methodology to characterize the structural features of biologics. Forced oxidative stress studies are used to investigate the stability profile, to develop pharmaceutical formulations and analytical methods. Here, the effects of forced oxidative stress by H_2O_2 on the monoclonal antibody Abituzumab have been characterized by a multianalytical approach combining NMR spectroscopy, mass spectrometry, differential scanning calorimetry, surface plasmon resonance, computational tools, and bioassays. This integrated strategy has provided qualitative and semiquantitative characterization of the samples and information at residue level of the effects that oxidation has on the HOS of Abituzumab, correlating them to the loss of the biological activity.

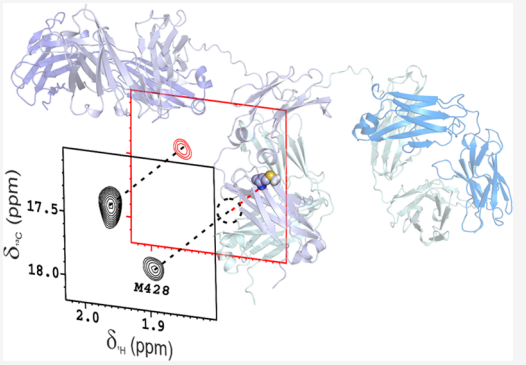

Forced degradation studies (stress testing) are a key step for assessing protein degradation pathways in the development of biologics. This information is, in turn, capital for the evaluation of drug stability and the related impact on purity, potency, and safety.[1,2] Under the quality-by-design (QbD) paradigm, formulation studies may benefit from the development of analytical methods, support of specification setting, and characterization of the degradation routes of formulation components under various stress circumstances.[3]

Critical quality attributes (CQA) are physical, chemical, biological, or microbiological properties or characteristics that must fall within appropriate limits, ranges, or distributions to ensure the optimal product quality.[3] Forced degradation studies provide the punctual characterization of the molecule's CQA that may be subjected to modifications following selected stress. Among CQA, special focus is devoted to the higher-order structure (HOS: secondary, tertiary, and quaternary structure). This is because the HOS of a protein is a fingerprint that covers structural quality attributes potentially linked to the function of the molecule. It is therefore a key determinant for an indepth understanding of the structure−function relationship.

Currently, there is no single approach for comprehensive evaluation of HOS: typical techniques CD, hydrogen/deuterium exchange-mass spectrometry (HDX-MS), fluorescence, Fourier-transform infrared spectroscopy (FT-IR), Raman spectroscopy, and thermal analysis by Nano-DSC measure different aspects of the structure, either directly or indirectly. With the exception of HDX-MS, these low-resolution techniques are not sensitive enough to small and local changes in the protein fold. Indeed, very small perturbations of the protein structure—in particular, those ascribable to post-translational modifications (PTMs), such as oxidation or deamidation—are extremely challenging to measure confidently/reproducibly using traditional spectroscopic technologies, especially in complex formulation or in case of samples containing additives. NMR, on the contrary, can provide detailed characterization of the structure of a biologic, starting from the early phase of development,[4−8] that grants a broad range of applications in pharmaceutical development.[9,10] In particular, because of its high sensitivity to structural changes and resolution, NMR is among the best available techniques to characterize the HOS of biotherapeutics.[4−6,11−15] Moreover, NMR virtually does not require sample manipulation and the spectra can be recorded directly on the final pharmaceutical product.

A recent study has shown that NMR of mAbs is highly reproducible even between different laboratories[6] and this reproducibility makes NMR data ideally suited for statistical analysis. A number of different statistical comparison strategies

Received: January 20, 2023
Accepted: May 16, 2023
Published: June 6, 2023

https://doi.org/10.1021/acs.analchem.3c00317
Anal. Chem. 2023, 95, 9199−9206

are currently available in the literature. PCA[16] and NMR-based PROFILE[17,18] analysis are usually performed on 1D ^{1}H spectra. Comparison of peak lists of 2D NMR spectra is also an established method to detect changes in HOS.[19] Combined chemical shift deviation (CCSD)[11,20,21] gives a quantitative measure of similarity. Creating peak lists in these spectra is challenging, but the spectrum can be used as a fingerprint, e.g., spectral similarity by correlation or easy comparability of HOS (ECHOS).[15,22] Multivariate statistical analysis methods compare groups of spectra and account for variations within different groups.[20,21,23]

Abituzumab (DI17E6) is a humanized monoclonal IgG2 antibody that selectively binds to the αv extracellular domain of integrins[24] that are overexpressed on a variety of tumor cells. The binding of Abituzumab to integrins blocks pathways involved in cell growth, motility, cell invasion, and tumor growth, interfering also with ion channels and actin intracellular cytoskeleton organization.[25,26] Here, Abituzumab is used as a model to test a new analytical workflow that integrates NMR spectroscopy with well-established biophysical techniques, biological assays, and recent computational methodologies. This new workflow was used to assess, quantify, and analyze the alterations of the structural and functional properties of this monoclonal antibody upon forced oxidative stress. This commonly investigated degradation pathway can be appropriately induced in biopharmaceutical products by treating them with an oxidizing agent, H_2O_2[1,27] in this case. We use it here to correlate the structural changes to the altered biological activity.

EXPERIMENTAL SECTION

Oxidative Stress Protocol. The oxidative stress conditions (0.1% H_2O_2 for 60 min at room temperature) were selected on the basis of the existing literature,[1,27] the treatment was performed by adding 100 μL of 1% H_2O_2 to 900 μL of the formulated mAb (active principle 25 mg/mL. Placebo: sodium chloride 50 mM, sucrose 150 mM, citric acid monohydrate 10 mM, Tween 80 0.1% w/v, pH 6.0). After 1 h of incubation at room temperature, methionine (40 mg) was added to quench the reaction. Eventually, the buffer was exchanged back to the formulation one using a PD10 column. This procedure did not induce any modification in aggregation or protein concentration, as detected by SEC-MALS experiments and OD measurements (Table S1).

NMR Spectroscopy. All NMR samples were prepared by adding in a 5 mm NMR tube 60 μL of $^{2}H_2O$ to 540 μL of the formulated mAb (untreated or oxidized). Spectra were recorded on a Bruker AVANCE NEO spectrometer operating at 900 MHz (^{1}H Larmor Frequency) and equipped with a TCI cryo-probe. Temperature was regulated to 313 K. 1D ^{1}H spectra were acquired with presaturation to suppress the water signal (zgpr), with 128 and an interscan delay of 4 s. 2D spectra were acquired using the band-selective ^{1}H−^{13}C ALSOFAST HMQC sequence[12,13,20,28] with and without SIERRA[13] suppression of excipient signals (^{1}H spectral window = 19.9 ppm; ^{13}C spectral window = 30 ppm; interscan delay = 0.25 s; number of scans = 512; number of points in F1 dimension = 256). The statistical analysis of 1D spectra was performed using the PROFILE[17,18] and PCA routines in MestReNova v14.2.2-28739 (MestreLab), while the analysis of 2D ^{1}H−^{13}C ALSOFAST HMQC spectra was performed using the MBioHOS plugin in MestReNova v14.2.2-28739 (MestreLab). More in detail, the chemometric analysis was based on two algorithms available in the software: CCSD[19] and ECHOS.[22]

Reducing Peptide Mapping by LC-MS. The sample preparation is based on reduction, alkylation, and enzymatic hydrolysis by either trypsin or chymotrypsin. Hydrolyzed samples were then analyzed by LC-MS on an Orbitrap Fusion Lumos system. The column used for chromatographic separation was an Acquity UPLC BEH C18, 1.7 μm, 2.1 μm × 100 mm (waters) and the mass spectrometer was operated in DDA mode. The column temperature was set to +60 ± 2 °C and the autosampler to +5 ± 3 °C. Mobile phases were composed of 0.1% formic acid in Milli-Q Water (Mobile phase A) and of 0.1% formic acid in ACN (Mobile phase B). The separation was achieved by an 80 min gradient with the variable slope starting from 2% B with a flow rate of 0.4 mL/min. UV acquisition was carried out at 214 nm. The mass spectrometer capillary voltage was set at 3500 V, with the sheath gas set at 50, the Aux gas set at 10, the Sweep gas at 2, and the temperature of both the ion transfer tube and the vaporizer set at 350 °C. The full scan was operated over a m/z range between 250 and 2000 at a resolution of 60 000, setting the AGC target at 4.0e5, maximum injection time at 150, and employing a dynamic exclusion of 1.6 s. The MS/MS data was acquired at a resolution of 30 000, setting the AGC target at 5.0e4, the maximum injection time at 150 ms, and the HCD collision energy at 28%. The data was then searched using Expressionist MS Refiner (Genedata).

Experimental methods for differential scanning calorimetry (DSC), cell-based potency assay, and binding affinity to FcRn are described in the Supporting Information.

RESULTS

HOS Characterization by NMR Spectroscopy. NMR characterization of the HOS of Abituzumab upon oxidative stress was carried out by using 1D and 2D NMR spectra. For 2D experiments, we chose to use the strategy proposed by Arbogast et al.[15] by acquiring methyl-edited ^{1}H−^{13}C ALSOFAST HMQC spectra because the fast rotation of methyl groups around their symmetry axis ensures intense and well-resolved NMR signals even for larger protein therapeutics. These spectra are also used for the analysis of the HOS in small protein therapeutics because they represent a good compromise between information content and acquisition times. All 2D NMR spectra were acquired on the intact mAb in its formulation buffer to avoid any sample manipulation.

2D ^{1}H−^{13}C methyl ALSOFAST HMQC band-selective experiments[12−14,20,28] (Figure S1A) allow for preferential excitation of a region of the spectrum (the methyl one) leaving the rest of the resonances unaffected. In this way, off-resonance signals of aliphatic excipients that mainly resonate outside this region (i.d Sucrose) do not experience an increase in signal intensity, and a fingerprint of the protein can be obtained. However, it may occur that excipients containing methyl groups resonating in this region (on-resonance signals) may cover the protein signals. Moreover, these excipients may introduce baseline distortions that can negatively influence the chemometric analysis or impact the fidelity of picked peak parameters in their vicinity. In these cases, selective pulsing techniques that suppress those interfering signals at specific ^{1}H−^{13}C frequency positions (selective excipient reduction and removal (SIERRA) filter) can be employed.[13]

In the spectra of our formulated mAb, only signals of Tween 80 resonate in the methyl region, one of those being very

https://doi.org/10.1021/acs.analchem.3c00317
Anal. Chem. 2023, 95, 9199−9206

intense. The intensity of this signal and the related baseline distortion were effectively reduced by using the SIERRA filter (Figure S1B). Overall, this filter only slightly affected the global signal intensity. The number of signals visible in the spectra, however, is lower than the 329 methyl resonances, expected from the protein sequence. 126 and 104 cross-peaks were identified by the automatic peak-picking procedure of Topspin 4.0.6 in the spectra acquired with and without the SIERRA filter, respectively. This is not surprising for spectra of an intact antibody because of the inherently broader linewidth of NMR signals in large proteins. Also, the microscopic viscosity of the medium is increased by the excipients in high concentrations, further increasing the line broadening.

Statistical analysis has been carried out on the spectrum acquired without the SIERRA filter, considering that it has been proved that the pattern of few signals is enough to monitor the HOS of the protein[21] and that multiplicative (t1-) noise in the Tween 80 signal yields artifacts when not filtered out through SIERRA.

1D ^{1}H and 2D ^{1}H−^{13}C ALSOFAST HMQC band-selective spectra recorded on the protein before and after the oxidative stress are reported in Figures 1 and S2. Chemical shift perturbations or changes in signal intensities are reporters of alterations in the HOS of the mAb after chemical modifications and/or conformational changes. As can be observed, the treatment induces appreciable changes in both 1D and 2D spectra: a decrease of the intensity is observed for some signals, together with the appearance of new cross-peaks. The analysis of the alterations observed in the 2D spectra provides interesting information on the structural effects of oxidation, contributing to explain the loss of activity observed for this oxidized antibody (see later). In particular, the signals belonging to the methyl groups of the methionine residues exhibit a well-defined range of chemical shifts and some of them are visible in the 2D ^{1}H−^{13}C spectra. After the treatment, these signals are extremely decreased in intensity, suggesting the occurrence of oxidation events at these sites (Figure 1C). Further, after oxidation, the integral of the signals is about half of the original value.

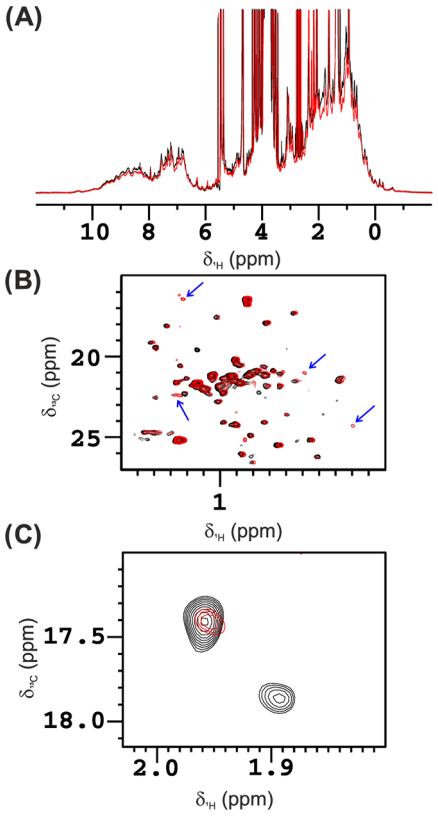

Figure 1. (A) Overlay of 1D ^{1}H spectra acquired with presaturation scheme for water suppression (zgpr), before (black) and after oxidative stress (red). (B) Region of 2D ^{1}H−^{13}C ALSOFAST HMQC band-selective spectra with SIERRA filter acquired before (black) and after oxidative stress (red). Blue arrows highlight some of the new cross-peaks appearing upon stress. (C) Region of the 2D ^{1}H−^{13}C ALSOFAST HMQC band-selective spectra with SIERRA filter, where the methyl signals of methionine residues resonate. The spectra were acquired before (black) and after (red) oxidative stress.

In order to assess the significance of the observed differences between the spectra before and after the treatment, statistical analysis was performed on 1D spectra by employing the PROtein Fingerprint by Line shape Enhancement (PROFILE) method.[17,18] This statistical method, being capable to discriminate antibody and excipient signals based on their different translational diffusion rates, allows a comparability assessment based on the mAb components of the spectrum only (Figure 2A). This analysis indicated that the structural alterations occurring upon oxidative stress were significant. The principal component analysis (PCA) confirms this result, highlighting a clear separation of untreated and treated samples on the PC2 axis (Figure 2B).

The statistical analysis on 2D spectra was performed by employing two different comparison algorithms built within the BiologicsHOS software, CCSD,[19] and ECHOS[22] (Figure 2C,D). Both methods provide an objective numerical assessment of structural comparability while pinpointing the spectroscopic reason/s for an observed difference. The two approaches can be considered complementary as the first one takes into consideration chemical shift perturbations, while the second one, variations in signal amplitudes. Further, the average CCSD obtained by comparing the 2D ^{1}H−^{13}C ALSOFAST HMQC spectra before and after oxidative stress is 4.72 ppb, a value based on the current literature[21,29,30] is apparently not indicative of significant differences (this algorithm measures the amount the peaks are shifted between two spectra, and considers 0 as a theoretical value corresponding to no shifts, i.e., identical samples). This result suggests that, globally, the fold of the protein is maintained after the stress condition since most of the cross-peaks have the same chemical shift in spectra acquired before and after the stress test (see also Figure S3). However, the CCSD algorithm was able to reassign only 34 signals in the spectrum acquired after the oxidative stress, with respect to the 73 signals identified by automatic peak-picking of the spectrum of untreated mAb. These signals were not detected by the program because of their drastic decrease in intensity, therefore suggesting the occurrence of changes on local regions of the protein. The ECHOS algorithm confirmed this observation as well. The method compares the amplitude of signals based on a linear regression, where the correlation coefficient R serves as a comparability/similarity indicator. The R value obtained in this comparison was 0.91, and in the plot, many points deviate far apart from the regression line, indicating significant statistical differences among the two samples in terms of intensity.

Eventually, the analysis of the protein fingerprint before and after oxidative stress was integrated by comparing the obtained

https://doi.org/10.1021/acs.analchem.3c00317
Anal. Chem. 2023, 95, 9199−9206

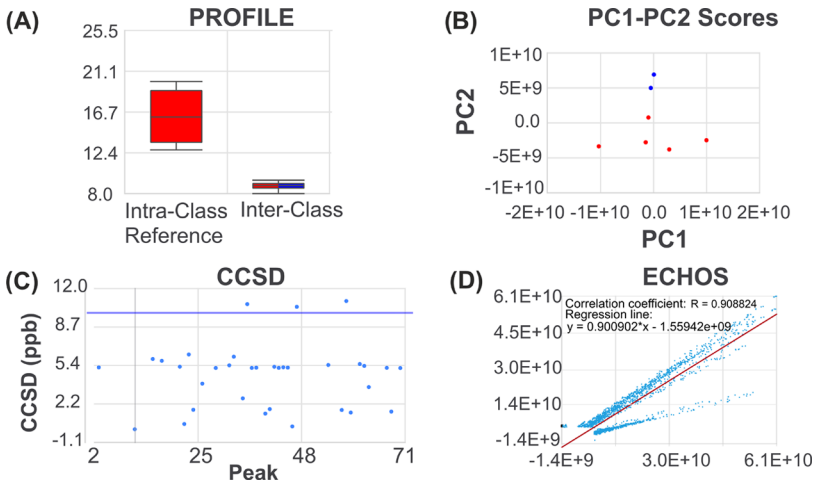

Figure 2. Statistical analysis performed using the (A) PROFILE method[17,18] and (B) principal component analysis (PCA) on 1D ^{1}H spectra acquired with a presaturation scheme only to suppress the water signal (five replicates of untreated material, red, versus two replicates of stressed material, blue): the excipient signals of the buffer were first subtracted and excluded from the analysis (blind regions: 5.7−2.5; 4.95−4.62; 4.4−3.4; 2.85−2.6; 2.41−2.34; 2.3−2.15; 2.1−2.0; 1.68−1.61; 1.45−1.3; 0.95−0.91 ppm). In the PROFILE method, variability between spectra is quantified by the value S(dB), the logarithmic scale of similarity: the higher the value, the higher the similarity. In the present comparison, the variability between groups (interclass box) does not overlap with in-group variabilities (intraclass box: red, untreated material), indicating statistically significant differences upon oxidative stress. (C, D) Statistical analysis of 2D ^{1}H−^{13}C ALSOFAST HMQC spectra before and after oxidative stress. (C) CCSD. The plot highlights which signals between the two spectra are the most dissimilar (*i.e.*, those peaks above the threshold shown by the horizontal blue line that is set at twice the standard deviation of the shift differences). (D) ECHOS. The plot shows how signals cluster around the regression line (red): the more similar the spectra are, the more the points will cluster around them.

spectra with the assignment for the immunoglobulin CH domains. The complete sidechains assignment is reported for the isolated CH3 domain of human IgG1 (bmrb: 15204[31]), while for the CH2 domain, only the backbone assignment is available (bmrb codes: 25224[32] and 15514[33]). The IgG1-based construct reported in the literature differs from that of the IgG2-based CH3 domain by three residues (D356E, L358M, and V397M), with only methionine 428 still present in the IgG2 protein. Interestingly, the frequencies assigned to the methyl group of Met-428 of IgG1 CH3 domain fits with a cross-peak in the 2D ^{1}H−^{13}C ALSOFAST HMQC spectrum of Abituzumab and could be tentatively assigned together with the signals of residues Thr-359, Ile-377, Ala-378, Leu-410, and Leu-432 (Figure 3). De novo resonance assignment of antibodies is challenging because of their size and difficulty in obtaining isotopic enrichment for the full-length construct. At the same time, assignment of the isolated domains has proven to be feasible,[31−33] and the presence of several conserved parts facilitates the analysis.

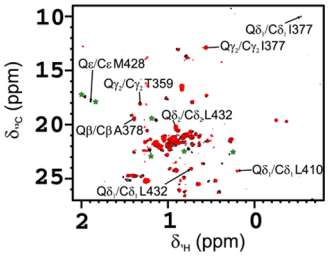

Figure 3. Region of the 2D ^{1}H−^{13}C ALSOFAST HMQC band-selective spectra acquired before (black) and after oxidative stress (red). The tentative assignment of some signals, obtained from the data reported in the bmrb (code: 15204[33]), has been indicated. The signals, for which assignment is not available but appear decreased in intensity after oxidation, have been marked with a green star.

The analysis of the NMR spectrum of Abituzumab reveals that at least six signals exhibit a decrease in intensity. Notably, one of the signals experiencing a decrease is Met-428. At the same time, the other five assigned residues of the CH3 domain (Thr-359, Ile-377, Ala-378, Leu-410, and Leu-432) do not experience any change in signal intensity, upon treatment with oxygen peroxide. The preservation of the signal intensity and the absence of chemical shift perturbation for these five residues, which are distributed in different regions of the CH3 domain, prove that oxidative stress does not affect the global folding of the protein, although it seems to affect local regions and probably the interaction with other proteins or domains within the whole antibody.

Evaluation of the Oxidation Sites by Reducing Peptide Mapping by LC-MS/MS. The effect of the oxidative stress on Abituzumab was assessed by reducing peptide mapping by LC-MS/MS with the aim to evaluate the degree of oxidation of the molecule's methionine residues. The results (Table 1) highlight that the applied oxidative conditions were

Table 1. Reducing Peptide Mapping by LC-MS/MS Results upon Oxidative Stress[a]

	methionine residue	untreated	oxidized sample
light chain	Met-4	0.13	0.26
heavy chain	Met-34	2.27	2.16
	Met-70 or Met-81	2.25	1.32
	Met-105	0.36	0.52
	Met-252	2.11	76.59
	Met-358	0.39	30.42
	Met-397	0.55	55.69
	Met-428	0.31	44.65

[a]The results for each residue (Eu numbering) are expressed as relative percentages with respect to the sum of all species detected for a specific peptide.

https://doi.org/10.1021/acs.analchem.3c00317
Anal. Chem. 2023, 95, 9199−9206

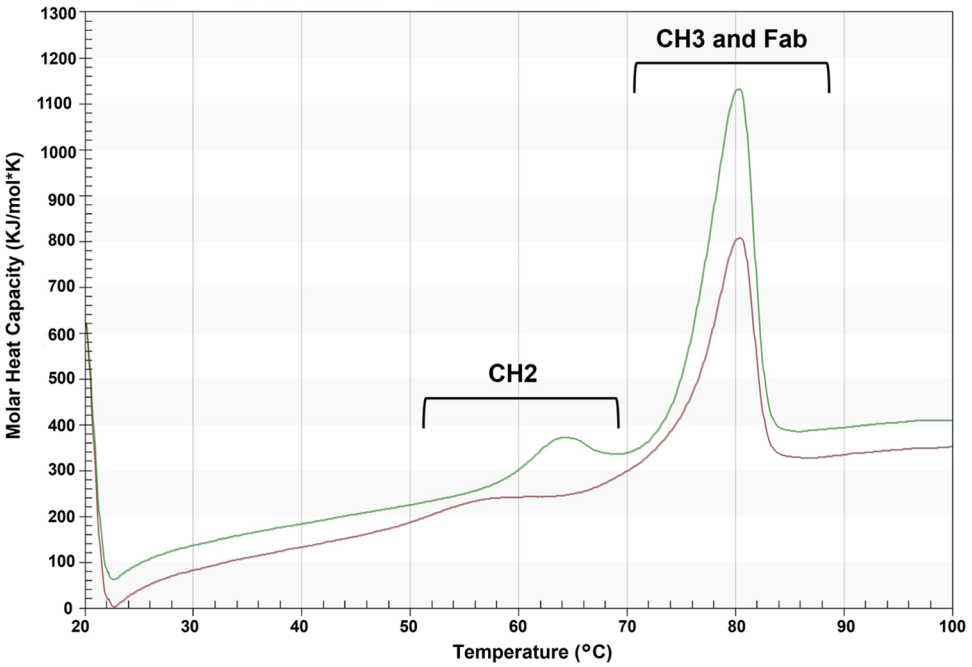

Figure 4. Stacked nano-DSC thermograms of untreated (green) and oxidized materials (red).

sufficient to induce strong oxidation of the molecule. Susceptibility to this PTM was observed only in case of four residues on the heavy chain: Met-252 (CH2 domain) and methionine residues 358, 397, and 428 on the CH3 domain. The other methionine residues remained unaffected (values are within method variability). Of note, Met-252, Met-358, and Met-428 are highly conserved residues among different IgG isotypes, while Met-397 is a conserved residue in the IgG2 antibody:[34] all of these residues were previously described as very susceptible to oxidation.[35−37]

Assessment of Thermal Stability by Nano-DSC. Treated samples were evaluated by nano-differential scanning calorimetry (DSC) in order to assess variations in terms of thermal stability upon oxidative stress, which could be indicative of conformational changes. Indeed, since the changes in Cp (heat capacity) measured by DSC originate from the disruption of the forces stabilizing native protein structures (hydrogen bonds and hydrophobic and electrostatic interactions), the calculated thermodynamic parameters are sensitive to the structural state of a biomolecule. As can be observed from the overlay of the thermograms reported in Figure 4, untreated and treated samples present three endothermic thermal transitions, each one corresponding to a domain of the molecule (CH2, CH3, and Fab), as typically observed in the case of IgGs.[38−40] As better highlighted in Figure S4 and Table S2, it is evident that thermal stability is affected by oxidation. Further, a consistent decrease correlating to the treatment is observed for Tm1 (CH2 domain) and partially for Tm2 (CH3 domain), while Tm3 (Fab domain) is overall unaffected.

Assessment of Biological Activity. The biological activity of the oxidized mAb, expressed as the ability of the Fab portion to bind its target, was investigated via bioassays. The results are described in Table S3 in terms of potency (%) and indicate that the Fab portion biological activity is not significantly affected by oxidation. Only when the biological activity of the Fc portion (that comprises the CH2 and CH3 domains) was investigated by SPR (Biacore) in terms of binding to the FcRn receptor, the effects induced by oxidation were observed. From Figure S5, it is possible to see that the oxidized sample sensorgram shows a strong decrease in terms of the signal with respect to the untreated sample, reflecting a decreased affinity to the target receptor.

DISCUSSION

The neonatal Fc receptor (FcRn) is widely known as responsible for the transfer of passive humoral immunity from the mother to the fetus in rodents and humans. In adults, they are involved in the cellular recycling of IgGs to extend their half-life in blood circulation.[41] These receptors are expressed quasi-ubiquitously, with a predominant localization at the intracellular level.[42] The remarkable reduction of the binding affinity of Abituzumab for the FcRn, which we observed upon oxidative treatment, is related to the modification of the protein HOS detected by NMR spectroscopy, MS, and Nano-DSC. These results agree with the current literature reporting that the main structural changes upon oxidation in IgG antibodies occur in the CH2−CH3 portion of the Fc domain.[35−37,43−46] Indeed, FcRn receptors bind the CH2−CH3 edge on the Fc domain of IgGs,[43] and it was previously observed that the oxidation of the conserved methionine residues, located in this region, has a strong impact on antibody binding affinity to neonatal receptors.[36,37,44] To further investigate these observations, a structural model of Abituzumab was generated with α-fold (AlphaFold2.ipynb).[47] The model has provided interesting hints for the analysis and interpretation of the experimental data. The calculated structure suggests that Met-252, Met-428, and Met-397 are located on flexible regions (loops or at the edge of secondary structure elements) and are therefore more sensitive to oxidation by H_2O_2, as previously reported.[48,49] Additionally, the computational model shows that Met-252 and Met-428 are close to the interface between the CH2 and CH3 domains of the Fc portion, which is crucial for the interaction with the FcRn receptor. Conversely, Met-397 and

https://doi.org/10.1021/acs.analchem.3c00317
Anal. Chem. 2023, 95, 9199−9206

Met-458 are away from the FcRn binding site[50] and are not involved in the stabilization of the CH2−CH3 interface. As a consequence, oxidation of Met-397 and Met-458 does not appear to significantly affect either the binding or the thermal stability[36,44,51] of the Fc fragment. These observations agree with the LC-MS/MS and DSC experimental data. Indeed, according to LC-MS/MS results, higher oxidation after treatment with H_2O_2 has been observed in the case of the above-discussed four methionine residues (Met-252, Met-397, Met-428, and Met-458). The other five methionine residues of the protein (Met-4, Met-34, Met-70, Met-81, and Met-105) are located on β-strands of the Fab portion of the mAb and display lower susceptibility to oxidation. Also, the alteration of the thermal stability experienced mainly by the CH2 domain and the lower effects observed for CH3 and Fab domains, perfectly correlate with the LC-MS/MS results. In this respect, it has been reported that the oxidation of Met-252 directly affects the FcRn/IgG binding, while the oxidation of Met-428 is supposed to destabilize the CH2−CH3 hinge region by weaking the interaction between CH2 and CH3.[37,45] Moreover, it has been described by O'Connor, Ionescu, and coworkers that Met-252 and Met-428 oxidation is accompanied by conformational changes in the CH2 domain (between residues 242 and 252),[35,46] whereas the structure of the CH3 domain is less compromised. Data also agree with the reduced binding affinity of the oxidized mAb toward the FcRn and the unaffected biological activity toward the target of the Fab portion.

CONCLUSIONS

Oxidation is a common degradation pathway for biologics, and forced oxidative stress studies are employed to optimize therapeutic formulations and to set up robust control strategies during drug development. The NMR analysis integrated in a traditional analytical workflow permits a detailed comparability study, providing information on the protein experiencing degradation and details on the structural effects induced by stress. In a previous study, Solomon et al.[52] demonstrated the high degree of correlation between NMR and techniques routinely used in pharmaceutical development. In this study, we demonstrate that this approach complemented with MS analysis can be applied also to more complex systems, i.e., intact mAbs in excipient-rich formulations. Furthermore, even when relying on NMR pulse sequences with lower resolution (that are necessary to study complex samples), the orthogonality between different analytical techniques is maintained. The NMR fingerprint of the methyl-groups region, obtained by the analysis of 1D ^{1}H spectra and 2D $^{1}H-^{13}C$ correlation spectra, allowed us to fast assess the HOS alteration and provided qualitative and semiquantitative information on the effects of oxidation on Abituzumab. The extent of the change in intensity affecting the signals of the two methionines and the corresponding effect observed in the peptide mapping analysis indicate that about half of the macromolecules in solution experience degradation on these two residues. However, the NMR data and nano-DSC results taken together point toward the preservation of the global folding of Abituzumab after oxidation and the presence of minor structural changes that however affect the biological function. The correlation of the NMR data with the peptide mapping analysis and biological assay results shed light on the possible specific local structural alterations responsible for the loss of the biological activity of Abituzumab upon degradation. When the assignment is available, NMR shows at atomic detail whether the local alterations affect other specific regions of the protein, allowing for the full potential of structural biology to be exploited, thus making it possible to follow a structure-based approach to increase the stability and avoid the loss of activity of biologics. In this respect, the design of possible specific mutants driven by this integrated workflow, as well as the change of the formulation components, represents a promising strategy to improve the stability and, more in general, the structure-based quality design of biotherapeutics.

ASSOCIATED CONTENT

Supporting Information

The Supporting Information is available free of charge at https://pubs.acs.org/doi/10.1021/acs.analchem.3c00317.

DSC and biological assays methods and results; additional NMR data; SEC-MALS; and OD data (PDF)

AUTHOR INFORMATION

Corresponding Authors

Marco Fragai − *Magnetic Resonance Centre (CERM), University of Florence, 50019 Sesto Fiorentino, Italy; Consorzio Interuniversitario Risonanze Magnetiche di Metalloproteine (CIRMMP), 50019 Sesto Fiorentino, Italy; Department of Chemistry "Ugo Schiff", University of Florence, 50019 Sesto Fiorentino, Italy;* orcid.org/0000-0002-8440-1690; Email: fragai@cerm.unifi.it

Fabio Baroni − *Analytical Development Biotech Department, Merck Serono S.p.a, an affiliate of Merck KGaA, Darmstadt, Germany, 00012 Guidonia, Italy;* orcid.org/0000-0002-8667-3251; Email: fabio.baroni@emdgroup.com

Authors

Linda Cerofolini − *Magnetic Resonance Centre (CERM), University of Florence, 50019 Sesto Fiorentino, Italy; Consorzio Interuniversitario Risonanze Magnetiche di Metalloproteine (CIRMMP), 50019 Sesto Fiorentino, Italy; Department of Chemistry "Ugo Schiff", University of Florence, 50019 Sesto Fiorentino, Italy*

Enrico Ravera − *Magnetic Resonance Centre (CERM), University of Florence, 50019 Sesto Fiorentino, Italy; Consorzio Interuniversitario Risonanze Magnetiche di Metalloproteine (CIRMMP), 50019 Sesto Fiorentino, Italy; Department of Chemistry "Ugo Schiff", University of Florence, 50019 Sesto Fiorentino, Italy; Florence Data Science, University of Florence, 50134 Florence, Italy;* orcid.org/0000-0001-7708-9208

Christian Fischer − *Bruker BioSpin GmbH, 76275 Ettlingen, Germany*

Andrea Trovato − *Analytical Development Biotech Department, Merck Serono S.p.a, an affiliate of Merck KGaA, Darmstadt, Germany, 00012 Guidonia, Italy*

Francesca Sacco − *Magnetic Resonance Centre (CERM), University of Florence, 50019 Sesto Fiorentino, Italy*

Wolf Palinsky − *Biotech Development Programme, Merck Biopharma, an affiliate of Merck KgaA, Darmstadt, Germany, 1170 Aubonne, Switzerland*

Gabriella Angiuoni − *Analytical Development Biotech Department, Merck Serono S.p.a, an affiliate of Merck KGaA, Darmstadt, Germany, 00012 Guidonia, Italy*

Complete contact information is available at:

https://doi.org/10.1021/acs.analchem.3c00317
Anal. Chem. 2023, 95, 9199−9206

https://pubs.acs.org/10.1021/acs.analchem.3c00317

Author Contributions

This manuscript was written through contributions of all authors.

Funding

This work has been supported by Regione Toscana (CERM-TT, BioEnable); the Italian Ministero dell'Istruzione, dell'Università e della Ricerca through "Progetto Dipartimenti di Eccellenza 2023−2027 (DICUS2.0)"; the Recombinant Proteins JOYNLAB Laboratory; and the project FISR2021_-SYLCOV. The project "Potentiating the Italian Capacity for Structural Biology Services in Instruct-ERIC-ITACA.SB" (Project No. IR0000009) within the call MUR 3264/2021 PNRR M4/C2/L3.1.1 was funded by the European Union NextGenerationEU.

Notes

The authors declare the following competing financial interest(s): This research was performed using as case study sample a product in development by the healthcare business of Merck KGaA, Darmstadt, Germany. While the Company filed for patent protection regarding the product in development, no patents or patent applications have been filed for the technology described in this manuscript. Fabio Baroni, Andrea Trovato, Gabriella Angiuoni and Wolf Palinsky are employees of the healthcare business of Merck KGaA, Darmstadt, Germany.

■ ACKNOWLEDGMENTS

The authors acknowledge Angela Capolupo, Irene Benni, and Rowena Tufino. Furthermore, the authors thank Bruker (Francesca Benevelli and Daniel Mathieu) and MestreLab (Michael Bernstein) for the support. The authors acknowledge the support and use of resources of Instruct-ERIC, a landmark ESFRI Project, and specifically the CERM/CIRMMP Italy Centre. The authors also acknowledge H2020-INFRAIA iNEXT-Discovery.

■ REFERENCES

(1) Halley, J.; Chou, Y. R.; Cicchino, C.; Huang, M.; Sharma, V.; Tan, N. C.; Thakkar, S.; Zhou, L. L.; Al-Azzam, W.; Cornen, S.; Gauden, M.; Gu, Z.; Kar, S.; Lazar, A. C.; Mehndiratta, P.; Smith, J.; Sosic, Z.; Weisbach, P.; Stokes, E. S. E. *J. Pharm. Sci.* **2020**, *109*, 6−21.

(2) EMA. ICH Q5C Stability Testing of Biotechnological/Biological Products, European Medicines Agency. https://www.ema.europa.eu/en/ich-q5c-stability-testing-biotechnologicalbiological-products. (accessed 2022-10-12).

(3) Anonymous. ICH Q8 (R2) Pharmaceutical Development, European Medicines Agency. https://www.ema.europa.eu/en/ich-q8-r2-pharmaceutical-development. (accessed 2021-09-01).

(4) Arbogast, L. W.; Delaglio, F.; Schiel, J. E.; Marino, J. P. *Anal. Chem.* **2017**, *89*, 11839−11845.

(5) Elliott, K. W.; Ghasriani, H.; Wikström, M.; Giddens, J. P.; Aubin, Y.; Delaglio, F.; Marino, J. P.; Arbogast, L. W. *Anal. Chem.* **2020**, *92*, 6366−6373.

(6) Brinson, R. G.; Marino, J. P.; Delaglio, F.; Arbogast, L. W.; Evans, R. M.; Kearsley, A.; Gingras, G.; Ghasriani, H.; Aubin, Y.; Pierens, G. K.; Jia, X.; Mobli, M.; Grant, H. G.; Keizer, D. W.; Schweimer, K.; Ståhle, J.; Widmalm, G.; Zartler, E. R.; Lawrence, C. W.; Reardon, P. N.; Cort, J. R.; Xu, P.; Ni, F.; Yanaka, S.; Kato, K.; Parnham, S. R.; Tsao, D.; Blomgren, A.; Rundlöf, T.; Trieloff, N.; Schmieder, P.; Ross, A.; Skidmore, K.; Chen, K.; Keire, D.; Freedberg, D. I.; Suter-Stahel, T.; Wider, G.; Ilc, G.; Plavec, J.; Bradley, S. A.; Baldisseri, D. M.; Sforça, M. L.; Zeri, A. C.; de, M.; Wei, J. Y.; Szabo, C. M.; Amezcua, C. A.; Jordan, J. B.; Wikström, M. *MAbs* **2019**, *11*, 94−105.

(7) Rizzo, D.; Cerofolini, L.; Giuntini, S.; Iozzino, L.; Pergola, C.; Sacco, F.; Palmese, A.; Ravera, E.; Luchinat, C.; Baroni, F.; Fragai, M. *J. Am. Chem. Soc.* **2022**, *144*, 10006−10016.

(8) Rizzo, D.; Cerofolini, L.; Pérez-Ràfols, A.; Giuntini, S.; Baroni, F.; Ravera, E.; Luchinat, C.; Fragai, M. *Anal. Chem.* **2021**, *93*, 11208−11214.

(9) Phyo, P.; Zhao, X.; Templeton, A. C.; Xu, W.; Cheung, J. K.; Su, Y. *Adv. Drug Delivery Rev.* **2021**, *174*, 1−29.

(10) Kiss, R.; Fizil, Á.; Szántay, C. *J. Pharm. Biomed. Anal.* **2018**, *147*, 367−377.

(11) Arbogast, L. W.; Brinson, R. G.; Marino, J. P. *Anal. Chem.* **2015**, *87*, 3556−3561.

(12) Brinson, R. G.; Ghasriani, H.; Hodgson, D. J.; Adams, K. M.; McEwen, I.; Freedberg, D. I.; Chen, K.; Keire, D. A.; Aubin, Y.; Marino, J. P. *J. Pharm. Biomed. Anal.* **2017**, *141*, 229−233.

(13) Arbogast, L. W.; Delaglio, F.; Tolman, J. R.; Marino, J. P. *J. Biomol. NMR* **2018**, *72*, 149−161.

(14) Arbogast, L. W.; Delaglio, F.; Brinson, R. G.; Marino, J. P. *Curr. Protoc. Protein Sci.* **2020**, *100*, No. e105.

(15) Arbogast, L. W.; Brinson, R. G.; Formolo, T.; Hoopes, J. T.; Marino, J. P. *Pharm. Res.* **2016**, *33*, 462−475.

(16) Chen, K.; Long, D. S.; Lute, S. C.; Levy, M. J.; Brorson, K. A.; Keire, D. A. *J. Pharm. Biomed. Anal.* **2016**, *128*, 398−407.

(17) Poppe, L.; Jordan, J. B.; Lawson, K.; Jerums, M.; Apostol, I.; Schnier, P. D. *Anal. Chem.* **2013**, *85*, 9623−9629.

(18) Poppe, L.; Jordan, J. B.; Rogers, G.; Schnier, P. D. *Anal. Chem.* **2015**, *87*, 5539−5545.

(19) Williamson, M. P. *Prog. Nucl. Magn. Reson. Spectrosc.* **2013**, *73*, 1−16.

(20) Haxholm, G. W.; Petersen, B. O.; Malmstrøm, J. *J. Pharm. Sci.* **2019**, *108*, 3029−3035.

(21) Brinson, R. G.; Arbogast, L. W.; Marino, J. P.; Delaglio, F. *J. Chem. Inf. Model.* **2020**, *60*, 2339−2355.

(22) Amezcua, C. A.; Szabo, C. M. *J. Pharm. Sci.* **2013**, *102*, 1724−1733.

(23) Ghasriani, H.; Hodgson, D. J.; Brinson, R. G.; McEwen, I.; Buhse, L. F.; Kozlowski, S.; Marino, J. P.; Aubin, Y.; Keire, D. A. *Nat. Biotechnol.* **2016**, *34*, 139−141.

(24) Élez, E.; Kocáková, I.; Höhler, T.; Martens, U. M.; Bokemeyer, C.; Van Cutsem, E.; Melichar, B.; Smakal, M.; Csőszi, T.; Topuzov, E.; Orlova, R.; Tjulandin, S.; Rivera, F.; Straub, J.; Bruns, R.; Quaratino, S.; Tabernero, J. *Ann. Oncol.* **2015**, *26*, 132−140.

(25) Hamidi, H.; Ivaska, J. *Nat. Rev. Cancer* **2018**, *18*, 533−548.

(26) Goodman, S. L.; Picard, M. *Trends Pharmacol. Sci.* **2012**, *33*, 405−412.

(27) Tamizi, E.; Jouyban, A. *Eur. J. Pharm. Biopharm.* **2016**, *98*, 26−46.

(28) Rößler, P.; Mathieu, D.; Gossert, A. D. *Angew. Chem., Int. Ed.* **2020**, *59*, 19329−19337.

(29) Wang, D.; Zhuo, Y.; Karfunkle, M.; Patil, S. M.; Smith, C. J.; Keire, D. A.; Chen, K. *Molecules* **2021**, *26*, 4251.

(30) Cantini, F.; Andreano, E.; Paciello, I.; Ghini, V.; Berti, F.; Rappuoli, R.; Banci, L. *Pharmaceutics* **2022**, *14*, 1981.

(31) Liu, D.; Cocco, M.; Matsumura, M.; Ren, D.; Becker, B.; Remmele, R. L.; Brems, D. N. *Biomol. NMR Assignments* **2007**, *1*, 93−94.

(32) Yagi, H.; Zhang, Y.; Yagi-Utsumi, M.; Yamaguchi, T.; Iida, S.; Yamaguchi, Y.; Kato, K. *Biomol. NMR Assignments* **2015**, *9*, 257−260.

(33) Liu, D.; Cocco, M. J.; Rosenfied, R.; Lewis, J. K.; Ren, D.; Li, L.; Remmele, R. L.; Brems, D. N. *Biomol. NMR Assignments* **2007**, *1*, 233−235.

(34) Jefferis, R.; Lefranc, M.-P. *MAbs* **2009**, *1*, 332−338.

(35) Wang, W.; Vlasak, J.; Li, Y.; Pristatsky, P.; Fang, Y.; Pittman, T.; Roman, J.; Wang, Y.; Prueksaritanont, T.; Ionescu, R. *Mol. Immunol.* **2011**, *48*, 860−866.

(36) Bertolotti-Ciarlet, A.; Wang, W.; Lownes, R.; Pristatsky, P.; Fang, Y.; McKelvey, T.; Li, Y.; Li, Y.; Drummond, J.; Prueksaritanont, T.; Vlasak, J. *Mol. Immunol.* **2009**, *46*, 1878−1882.
(37) Stracke, J.; Emrich, T.; Rueger, P.; Schlothauer, T.; Kling, L.; Knaupp, A.; Hertenberger, H.; Wolfert, A.; Spick, C.; Lau, W.; Drabner, G.; Reiff, U.; Koll, H.; Papadimitriou, A. *MAbs* **2014**, *6*, 1229−1242.
(38) Garber, E.; Demarest, S. J. *Biochem. Biophys. Res. Commun.* **2007**, *355*, 751−757.
(39) Liu, D.; Ren, D.; Huang, H.; Dankberg, J.; Rosenfeld, R.; Cocco, M. J.; Li, L.; Brems, D. N.; Remmele, R. L. *Biochemistry* **2008**, *47*, 5088−5100.
(40) Ionescu, R. M.; Vlasak, J.; Price, C.; Kirchmeier, M. *J. Pharm. Sci.* **2008**, *97*, 1414−1426.
(41) Roopenian, D. C.; Akilesh, S. *Nat. Rev. Immunol.* **2007**, *7*, 715−725.
(42) Pyzik, M.; Sand, K. M.; Hubbard, J. J.; Andersen, J. T.; Sandlie, I.; Blumberg, R. S. *Front. Immunol.* **2019**, *10*, No. 1540.
(43) Martin, W. L.; West, A. P.; Gan, L.; Bjorkman, P. J. *Mol. Cell* **2001**, *7*, 867−877.
(44) Gao, X.; Ji, J. A.; Veeravalli, K.; Wang, Y. J.; Zhang, T.; Mcgreevy, W.; Zheng, K.; Kelley, R. F.; Laird, M. W.; Liu, J.; Cromwell, M. *J. Pharm. Sci.* **2015**, *104*, 368−377.
(45) Houde, D.; Peng, Y.; Berkowitz, S. A.; Engen, J. R. *Mol. Cell. Proteomics* **2010**, *9*, 1716−1728.
(46) Burkitt, W.; Domann, P.; O'Connor, G. *Protein Sci.* **2010**, *19*, 826−835.
(47) Jumper, J.; Evans, R.; Pritzel, A.; Green, T.; Figurnov, M.; Ronneberger, O.; Tunyasuvunakool, K.; Bates, R.; Žídek, A.; Potapenko, A.; Bridgland, A.; Meyer, C.; Kohl, S. A. A.; Ballard, A. J.; Cowie, A.; Romera-Paredes, B.; Nikolov, S.; Jain, R.; Adler, J.; Back, T.; Petersen, S.; Reiman, D.; Clancy, E.; Zielinski, M.; Steinegger, M.; Pacholska, M.; Berghammer, T.; Bodenstein, S.; Silver, D.; Vinyals, O.; Senior, A. W.; Kavukcuoglu, K.; Kohli, P.; Hassabis, D. *Nature* **2021**, *596*, 583−589.
(48) Shah, D. D.; Zhang, J.; Hsieh, M.; Sundaram, S.; Maity, H.; Mallela, K. M. G. *J. Pharm. Sci.* **2018**, *107*, 2789−2803.
(49) Shah, D. D.; Singh, S. M.; Mallela, K. M. *Pharm. Res.* **2018**, *35*, 232.
(50) Teplyakov, A.; Zhao, Y.; Malia, T. J.; Obmolova, G.; Gilliland, G. L. *Mol. Immunol.* **2013**, *56*, 131−139.
(51) Pan, H.; Chen, K.; Chu, L.; Kinderman, F.; Apostol, I.; Huang, G. *Protein Sci.* **2009**, *18*, 424−433.
(52) Solomon, T. L.; Delaglio, F.; Giddens, J. P.; Marino, J. P.; Yu, Y. B.; Taraban, M. B.; Brinson, R. G. *MAbs* **2023**, *15*, No. 2160227.

https://doi.org/10.1021/acs.analchem.3c00317
Anal. Chem. 2023, 95, 9199−9206